35th EPS Conference on Plasma Phys. Hersonissos, 9 - 13 June 2008 ECA Vol.**32D**, P-2.174 (2008)

Suppression of the Filamentation Instability by a Flow-Aligned Magnetic Field

A. Stockem[1], M. E. Dieckmann[2], R. Schlickeiser[1]

[1] *Theoretical Physics IV, Ruhr-University Bochum, Germany*

[2] *Department of Science and Technology (ITN), Linköping University, Norrköping, Sweden*

Introduction

The filamentation instability (FI) is a physical process which creates turbulent magnetic fields. It is applied to astrophysical scenarios like the plasma thermalization in the fast pulsar winds [1] or the production of the strong magnetic fields, which are required to explain the synchrotron emission in gamma-ray bursts [2, 3]. Another field of interest is the inertial confinement fusion, where a strong magnetic field could be important [4].

The aim of this work is to compare the results of analytical estimates with particle-in-cell (PIC) simulations of a system of two equal counterstreaming nonrelativistic cool electron beams propagating along a spatially homogeneous magnetic field [5]. The analytical predictions for the linear stage of the instability are mostly confirmed by the PIC simulations. Non-linear effects, which cannot be described by the analytics, yield interesting new results.

The physical process of the FI

The FI generally deals with two cool plasma beams moving in opposite directions. A small scale fluctuation of the magnetic field perpendicular to the flow deflects the charged plasma particles due to the Lorentz force. The particles are spatially separated and concentrated in current filaments. The magnetic fields induced by the currents amplify the initial fluctuations. The instability is stopped by a saturation mechanism, which is explained later. After this the current filaments merge and lead to a formation of a large scale perpendicular magnetic field.

Analytical Results

The anisotropic particle distribution function is given by

$$f(p_\perp, p_\parallel) = \frac{\delta(p_\perp)\, n}{2\pi\, p_\perp} \left[\delta(p_\parallel - m\gamma U) + \delta(p_\parallel + m\gamma U)\right] \tag{1}$$

where $p_\perp$ and $p_\parallel$ denote the perpendicular and parallel component of the relativistic particle momentum and m, n and U the electron mass, beam density and velocity, respectively. A linearisation and combination of the Vlasov and Maxwell equations provides the linear growth rate $\sigma(k)$ (Fig. 1). For $k \to \infty$ the linear growth rate is approximately constant

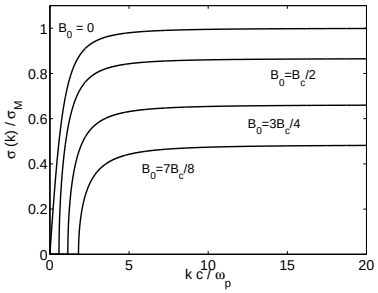

Figure 1: The linear growth rate of the FI.

$$\sigma_{max} = \sqrt{\frac{\omega_p^2}{\gamma}\frac{U^2}{c^2} - \Omega^2} \tag{2}$$

with $\Omega = eB_0/m$ [6]. The growth rate is reduced for an increasing B_0. No growth should occur at

$$B_0 = B_c = \frac{mU}{ec}\frac{\omega_p}{\gamma^{1/2}}. \tag{3}$$

The PIC Simulations

PIC simulations represent a collision-less kinetic plasma, which is equivalent to an incompressible phase space fluid that evolves under the influence of collective electric and magnetic fields. The coupled system of equations is given by the Maxwell equations (4) and the Lorentz equation (5)

$$\nabla \times \mathbf{E} = -\frac{\partial \mathbf{B}}{\partial t},\ \nabla \times \mathbf{B} = \mu_0 \varepsilon_0 \frac{\partial \mathbf{E}}{\partial t} + \mu_0 \mathbf{J}, \tag{4}$$

$$\frac{\mathrm{d}\mathbf{p}_{cp}}{\mathrm{d}t} = q_{cp}(\mathbf{E} + \mathbf{v}_{cp} \times \mathbf{B}) \tag{5}$$

which are solved with $\mathbf{p}_{cp} = m_{cp}\gamma\mathbf{v}_{cp}$, where $\mathbf{v}_{cp}$ is the velocity of a computational particle. The code we employ fulfills $\nabla \cdot \mathbf{E} = \rho/\varepsilon_0$ and $\nabla \cdot \mathbf{B} = 0$ to round-off precision. The boundary conditions of the simulations are periodic in all directions.

Long Term Magnetic Field Evolution

Fig. 2 shows the energy densities of the magnetic and electric field. The linear phase is well distinguishable from the non-linear phase and the same amplification level is reached for all B_0. Due to the saturation mechanism, the amplification of ε_E is delayed towards the amplification of ε_B.

ε_B grows also for $B_0 = B_c$ and a detailed analysis has shown that the amplification behaves completely different compared with the cases $B_0 < B_c$. This might be due to a temperature effect or a non-linear effect which allows particle diffusion across the magnetic field.

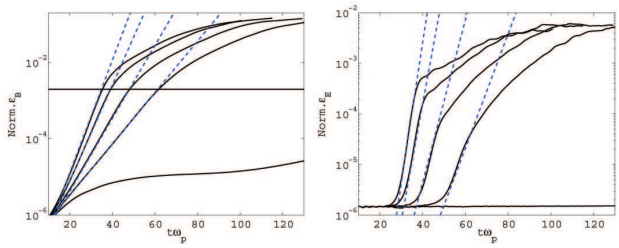

Figure 2: The energy densities of the magnetic (left) and electric field (right) for the different initial field strengths B_0.

The Linear Growth Rate

A Fourier transform of the field data allows a determination of the maximum linear growth rate. Fig. 3 shows the power spectra of the perpendicular magnetic field component for a constant wave number k_{max}, which shows the fastest growth of the instability during the linear phase, as $B_\perp^2(k_{max},t) \propto \exp(2\sigma t)$.

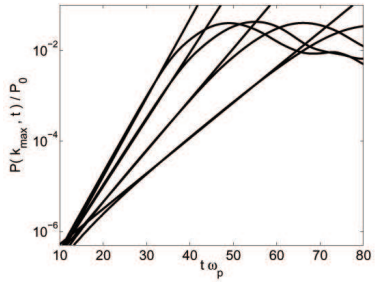

Figure 3: The linear power spectra of the perpendicular magnetic field for a constant wave number and varying B_0.

Straight lines are fitted to the simulation data in order to demonstrate the exponential behaviour. The growth rates of the simulations have been compared to the analytic estimated (Eq. (2)) and yield a deviance of 10% at most.

The Saturation Mechanism

The saturation mechanism is a result of the electron displacement by the magnetic pressure gradient, which has already been observed in a 1D simulation [7]. The amplification of the magnetic field is related to a magnetic pressure $P_b = B_\perp^2/2\mu_0$ in the perpendicular plane. The pressure gradient $\nabla P_b = B_\perp \nabla B_\perp/\mu_0$ pushes away the electrons, resulting in a space charge separation. This induces a restoring force which is proportional to the perpendicular electric field. For a constant wave number this results in $\nabla P_b \propto E_\perp \propto \exp(2\sigma t)$.

A cut through the perpendicular plane shows the minima of the gradient of $|B_\perp|$, and thus the

magnetic pressure which is proportional to $|B_\perp|^2$. They coincide with the minima of $E_\perp$. This confirms the magnetic pressure gradient to be the origin of the electric field.

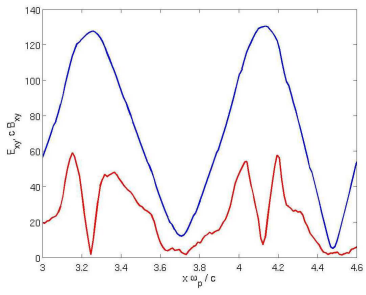

Figure 4: The minima of the gradient of $B_\perp$ coincide with the minima of $E_\perp$.

Conclusions

The comparison of PIC simulations and calculations for the linear phase of the FI shows an agreement between both methods. The analytic estimated growth rate has been confirmed by the simulations. Nevertheless, the simulations show an unexpected growth for $B_0 = B_c$, which we refer to a temperature or a non-linear effect due to particle diffusion across the magnetic field. The amplification levels of the magnetic and electric fields are independent of B_0 and a detailed analysis of the field data shows a connection between both fields leading to the saturation of the instability.

References

[1] Y. T. B. Yang, Y. Gallant, J. Arons and A. B. Langdon, Phys. Fluids B **5** 3369 (1993)

[2] M. V. Medvedev and A. Loeb, Astrophys. J. **526** 697 (1999)

[3] E. Waxman, Plasma Phys. Controll. Fusion **48** B137 (2006)

[4] M. E. Dieckmann, P. K. Shukla and B. Eliasson, New J. Phys. **8** 225 (2006)

[5] A. Stockem, M. E. Dieckmann and R. Schlickeiser, Plasma Phys. Controll. Fusion **50** 025002 (2008)

[6] A. Stockem, I. Lerche and R. Schlickeiser, ApJ **651** 584 (2006)

[7] G. Rowlands, M. E. Dieckmann and P. K. Shukla, New. J. Phys. **9** 247 (2007)